ANALYSIS AND OPTIMIZATION OF A VIBROACOUSTIC SYSTEM

Leandro Pavan, pavan@marcopolo.com.br
Marcopolo S. A., Divisão de Engenharia
Av. Rio Branco 4889, CEP 95060-650, Caxias do Sul – RS, Brasil

Walter Jesus Paucar Casas, walter.paucar.casas@ufrgs.br
Venâncio Lázaro Batalhone Neto, lazim.batalhone@gmail.com
Gustavo Batista Ribeiro, gbr00150@hotmail.com
Departmento de Engenharia Mecânica, Universidade Federal do Rio Grande do Sul
Rua Sarmento Leite 425, CEP 90050-170, Porto Alegre – RS, Brasil

Abstract. *The study of coupled problems considering the existence of some fluid-structure interaction, as the vibroacoustic problem, involves many open questions. The analysis and numerical optimization in vibroacoustic models, subject of this work, under defined boundary conditions, is important not only for understanding the physical phenomenon, but also to acquire sensitivity relative to the factors that influence the vibroacoustic response. The objectives of this work are: the exposition of a simple formulation for the modal analysis of vibroacoustic systems, the computational implementation of this formulation for comparison with results obtained from a commercial program, and to apply optimization. This work uses a system discretization with finite elements, by means of a non-symmetric matrix formulation u-p, in displacement u of the structure and pressure p of the fluid. After the modal analysis is realized, it is evaluated the numerical optimization of the structural mass. Some results are concerned with the pressure fringes in the fluid that match the structural deformation shape, which serve to verify if the structure or the fluid is predominant in the coupled mode. These results help to control the modal behaviour of a vibroacoustic system.*

Keywords*: Vibroacoustic, Coupled System, Fluid-Structure Interaction, Nonlinear optimization.*

1. INTRODUCTION

In a fluid-structure coupled system under dynamic excitation, the acoustic medium influences the behavior of the structure and vice versa. The vibration of the structure is influenced by the variation of the fluid pressure and the acoustic waves are sensible to the variation of the structural displacement. In the context of the free vibration, the natural frequencies and modes of the coupled system are different with reference to the uncoupled systems.

The energy in a coupled mode is divided between the structure and the fluid. Usually the largest amount of energy stays in the structure or in the fluid, from which the coupled system is classified as dominated by the structure or by the fluid (De Mello, 2003).

Usually, a mode dominated by the structure is originated by a structural uncoupled mode that induces an acoustic mode in the fluid. Equally, a mode dominated by the fluid is an acoustic mode that induces a mode in the structure. The fluid influences the movement of the structure through the pressure in the interface surface, as well as the movement of the interface surface modifies the acoustic domain.

The effect of the fluid pressure in the surface interface can be approximate through the term $\boldsymbol{f}_{s\Gamma_I}$, that is part of the excitement in the structural dynamic equation, constituted by the vectors of surface force and structural volume $(\boldsymbol{f}_{s\Gamma_I} + \boldsymbol{f}_{sB})$, according to Eqs. (1) and (2):

$$\boldsymbol{K}_{ss}\boldsymbol{u} + \boldsymbol{M}_{ss}\ddot{\boldsymbol{u}} = \boldsymbol{f}_{s\Gamma_I} + \boldsymbol{f}_{sB} \tag{1}$$

$$\boldsymbol{f}_{s\Gamma_I} = \int_0^L \boldsymbol{n}_s q \, dx \tag{2}$$

where $\boldsymbol{n_s}$ is the vector of structural shape functions. The forces in the interface surface of the structure are originated by the fluid action, being associated the normal component of the surface force q to the pressure distribution on the interface.

Considering the finite element method, it is possible to replace q by the expression of nodal polynomial approach for each finite element $\tilde{p} = \boldsymbol{n_f}^T \boldsymbol{p}$, where $\tilde{p}$ is the approach for the scalar field of local pressures, $\boldsymbol{n_f}$ is the vector of fluid shape functions, and $\boldsymbol{p}$ is the vector of nodal pressures of the element, and resulting the Eq. (3):

$$\boldsymbol{f}_{s\Gamma_I} = \int_0^L \boldsymbol{n}_s \boldsymbol{n}_f^T \, dx \; \boldsymbol{p} \tag{3}$$

that represents the equilibrium condition in the interface. Substituting Eq. (3) into Eq. (1) we obtain Eqs. (4) and (5):

$$\boldsymbol{K}_{ss}\boldsymbol{u} + \boldsymbol{M}_{ss}\ddot{\boldsymbol{u}} + \boldsymbol{K}_{sf}\boldsymbol{p} = \boldsymbol{f}_s \tag{4}$$

$$\boldsymbol{K}_{sf} = -\int_0^L \boldsymbol{n}_s \boldsymbol{n}_f^T \, dx \tag{5}$$

The coupling of the structural domain with the fluid domain is imposed in the normal direction $\hat{n}$ of the interface surface, through an identity that guarantees the cinematic compatibility:

$$\dot{\bar{\boldsymbol{v}}}_{\hat{\boldsymbol{n}}} = \ddot{\boldsymbol{u}}_{\hat{\boldsymbol{n}}} \tag{6}$$

that represents an slipping condition in the tangential direction to the interface.

Relative to the fluid domain, the fluid-structure coupling is described in terms of pressure variations in the neighborhood of the structural domain according to the interface boundary condition of Eq. (7), after using Eq. (6):

$$\frac{\partial p}{\partial \hat{n}} = -\rho_f \ddot{u}_{\hat{n}}, \quad \text{em}\,\Gamma_I \tag{7}$$

where ρ_f is the fluid density. Having substituted the component in the normal direction $\dot{\bar{v}}_{\hat{n}}$ by $\ddot{u}_{\hat{n}}$, and considering the expression $\ddot{\bar{u}} = \boldsymbol{n}_s^T \ddot{\boldsymbol{u}}$ to approximate the value of $\ddot{u}_{\hat{n}}$ by $\ddot{\bar{u}}_{\hat{n}}$, or in discretized way by $\boldsymbol{n}_s^T \ddot{\boldsymbol{u}}$, it results the Eq. (8):

$$\boldsymbol{M}_{ff}\ddot{\boldsymbol{p}} + \boldsymbol{K}_{ff}\boldsymbol{p} + \boldsymbol{M}_{fs}\ddot{\boldsymbol{u}} = \boldsymbol{f}_f \tag{8}$$

being the matrix with the interface terms expressed by Eq. (9):

$$\boldsymbol{M}_{fs} = \int_{\Gamma_I} \boldsymbol{n}_f \boldsymbol{n}_s^T \, d\Gamma_I \tag{9}$$

that allows to write the coupled system in its semi-discretized way. Rewriting Eqs. (4) and (8) together:

$$\boldsymbol{K}_{ss}\boldsymbol{u} + \boldsymbol{M}_{ss}\ddot{\boldsymbol{u}} + \boldsymbol{K}_{sf}\boldsymbol{p} = \boldsymbol{f}_s \tag{10}$$

$$\boldsymbol{M}_{ff}\ddot{\boldsymbol{p}} + \boldsymbol{K}_{ff}\boldsymbol{p} + \boldsymbol{M}_{fs}\ddot{\boldsymbol{u}} = \boldsymbol{f}_f \tag{11}$$

that allocated in a matrix, it generates the coupled formulation ***u-p*** in structural displacement and fluid pressure:

$$\begin{bmatrix} \boldsymbol{M}_{ss} & \boldsymbol{0} \\ \boldsymbol{M}_{fs} & \boldsymbol{M}_{ff} \end{bmatrix} \begin{Bmatrix} \ddot{\boldsymbol{u}} \\ \ddot{\boldsymbol{p}} \end{Bmatrix} + \begin{bmatrix} \boldsymbol{K}_{ss} & \boldsymbol{K}_{sf} \\ \boldsymbol{0} & \boldsymbol{K}_{ff} \end{bmatrix} \begin{Bmatrix} \boldsymbol{u} \\ \boldsymbol{p} \end{Bmatrix} = \begin{Bmatrix} \boldsymbol{f}_s \\ \boldsymbol{f}_f \end{Bmatrix} \tag{12}$$

For free vibrations, the second term of Eq. (12) is zero. The nonsymmetrical aspect of this formulation is its principal disadvantage, because it is not possible to use several efficient algorithms developed for symmetrical cases. The main advantage of this formulation is its reduced number of degrees of freedom to model the fluid domain, especially when compared with models based with more variables for the fluid domain.

2. STRUCTURAL OPTIMIZATION IN VIBROACOUSTIC SYSTEMS

This work looks for the dimensional optimization in vibroacoustic coupled systems, with the purpose of reducing the structural mass. The system is discretized with the finite element method, and the sequential quadratic programming SQP algorithm available in the software MSC.Nastran© is used for the optimization.

The structural domain is formed by plates, where the thickness is smaller with reference to the other dimensions. It is studied the optimization of the structural mass, and the thickness is chosen as the variable for the non linear optimization with constraints, although other choices are also possible, for example some properties of the fluid domain and characteristics associated to the connectivity.

Being *N* the order of certain frequency, the mass optimization is written so that two constraints are satisfied, the first is concerned with limits of the frequency *N* in Hz, and the second is concerned with minimum and maximum values of

the plates thickness, so that the solution must be technological and mathematically possible, because the thickness must have physical meaning.

The description of the optimization problem is defined by,

$$\begin{aligned} &\underset{\mathbf{x}\in\Re^r}{\text{Optimize}} && f = \text{Weight}(\mathbf{x}) \\ &\text{subject to:} && \omega_N^L \le \omega_N(\mathbf{x}) \le \omega_N^U \\ & && \mathbf{x}^{\text{mín}} \le x \le \mathbf{x}^{\text{máx}} \end{aligned}$$

where r is the number of structural elements, $\omega_N(\mathbf{x})$ is the N^{th} natural frequency exposed as function of the thicknesses vector $\mathbf{x}$ with lower ω_N^L and upper ω_N^U bounds respectively, $\mathbf{x}^{\text{mín}}$ is the vector of minimum thicknesses and $\mathbf{x}^{\text{máx}}$ is the vector of maximum thicknesses.

An optimization without constraints of the thickness can lead to singular points of value zero. Also, the constraint $\mathbf{x} \le \mathbf{x}^{máx}$ can be ignored after choosing a sufficiently large value of $\mathbf{x}^{máx}$, so that the inequality is always verified. During the optimization process, there is no explicit control over the modes crossing.

3. VIBROACOUSTIC SYSTEM: HEXAHEDRICAL CAVITY OVER A PLATE

Considering the model described in Msc.Software (1996), this system is studied for showing the coupling of modes when the frequencies of the decoupled structural and acoustic systems are closed for the interval of analyzed frequencies, as well as for optimizing the structural mass. The rectangular cavity has a height five times larger than the side of the base.

The software MSC.Nastran© is used for simulation and optimization of the coupled system, while the software MSC.Patran© is used for pre/post-processing the obtained results.

3.1. Square plate

The structure is a square plate for bending of side 20 in (0.508 m) and thickness 0.2 in (5,08 mm) supported in the four vertexes. The structural material is aluminum with the following properties: module of elasticity E=1.0x10^7 psi (68.948x10^9 N/m^2), Poisson's ratio ν=0.3 and density ρ=2.54 x10^{-4} lb-s^2/in^4 (2700 kg/m^3). Experimental and numerical studies with similar properties were conducted by Petyt and Mirza (1972) and Reid (1965).

The plate is discretized with a mesh (8x8), counting 64 two-dimensional elements *CQUAD4* of four nodes each and totaling 81 nodes. The boundary conditions are u=v=r_z=0 entirely in the plate. Additionally, it is considered the displacement of the vertexes equal to zero, z=0, as shown in Fig. 1.

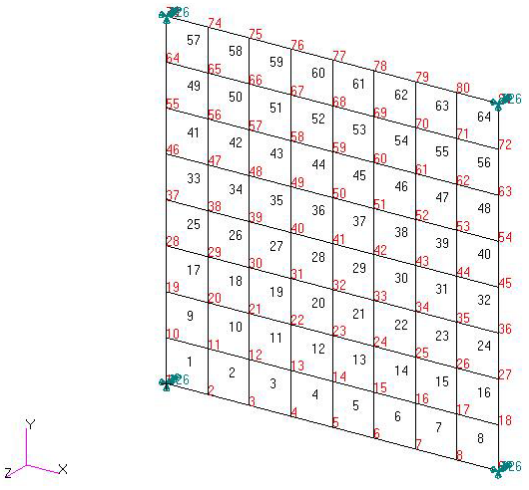

Figure 1. Mesh of the square shaped plate with indication of the boundary conditions

The natural frequencies are compared, in Tab. 1, with analytical solutions. The average variation of the results of MSC.Nastran© in relation to the analytical ones for the first two frequencies is 0.69%, value considered appropriate if observed that the maximum variation is only 0.39 Hz.

Table 1. Predicted frequencies in Hz of a square plate supported in the vertexes

Mode	Analytical (Blevins, 1995)	MEF MSC.Nastran©	Variation (%) MSC.Nastran© / analytical	Variation Hz MSC.Nastran© / analytical
1	34.02	34.41	1.15	0.39
2	75.50	75.67	0.23	0.17
3		75.67		
4		94.78		
5		191.56		
6		214.55		
7		252.84		
8		252.84		
9		343.86		
10		404.14		

It is observed in Fig. 2 two modes, the second and the third one, with different modal patterns but with identical frequencies because of the symmetry.

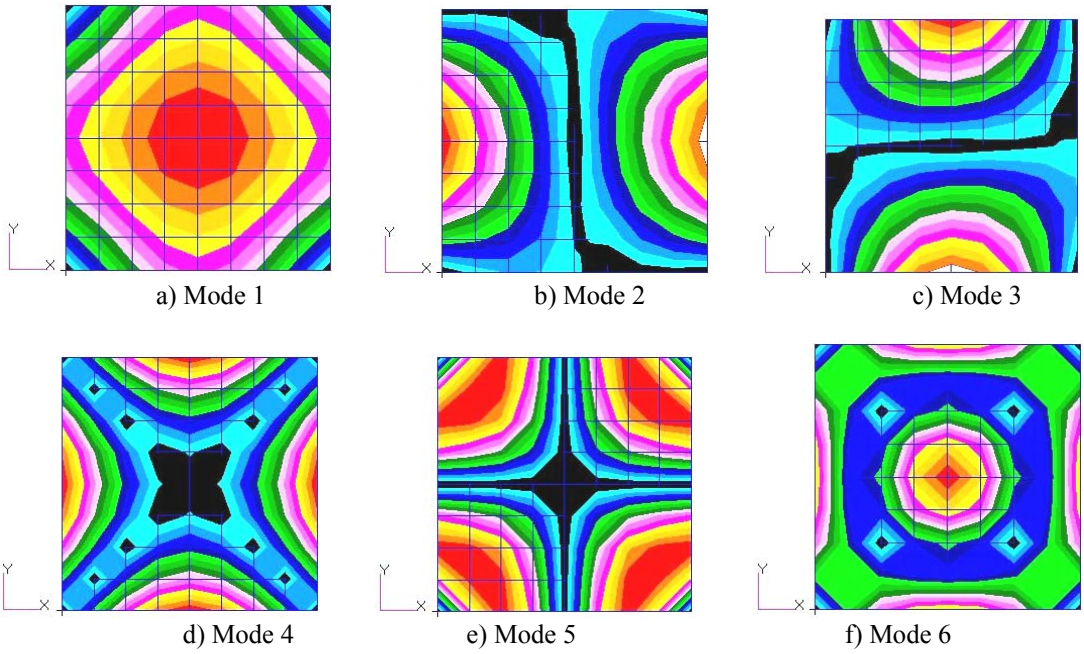

Figure 2. Modal patterns of the square plate supported in the vertexes

3.2. Hexahedrical acoustic cavity

The dimensions of the system are: sides of base equal to 20 in (0.508 m) and height equal to 100 in (2.54 m). The internal fluid is air with density ρ_f=1.21x10^{-7} lb-s^2/in^4 (1.29 kg/m^3) and sound velocity c_s=13000 in/s (330.2 m/s).

The cavity is discretized through a mesh (8x8x8) of hexahedrical solid elements CHEXA of 8 nodes each one, totaling 512 elements and 729 nodes. The boundary conditions correspond to rigid walls, Fig. 3.

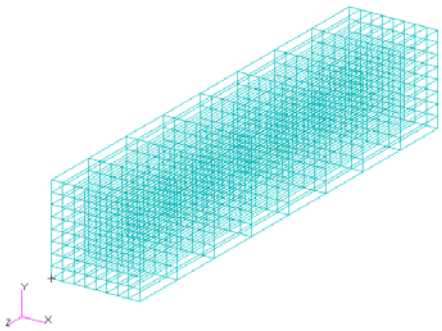

Figure 3. Mesh of the rectangular cavity with boundary conditions of rigid wall on faces

The obtained natural frequencies are compared, in Tab. 2, with analytical solutions according to Eq. (13), (Blevins, 1995); observing that the walls of the cavity are considered as rigid with infinite impedance.

$$f = \frac{c_s}{2}\sqrt{\left(\frac{i}{L_x}\right)^2 + \left(\frac{j}{L_y}\right)^2 + \left(\frac{k}{L_z}\right)^2} \qquad i = 0,1,2,\ldots;\ j = 0,1,2,\ldots;\ k = 0,1,2,\ldots \tag{13}$$

where,
f : natural frequency in Hz;
c_s : sound velocity at medium, in this case air, equal to 343.3 m/s;
L_x, L_y, L_z : length, width and height of the cavity.

The variation of the MSC.Nastran results relative to the analytical ones is 3.92% for the first twenty frequencies. The maximum difference is 38.2 Hz (11.52%) for the frequency of order 15. These set of results supplies sufficient conformity, especially for the first frequencies.

Table 2. Predicted frequencies of the hexahedrical acoustic cavity in Hz

Mode	Notation (i,j,k)	Analytical (Blevins, 1995)	MEF MSC.Nastran	Variation (%) MSC.Nastran / analytical	Variation Hz MSC.Nastran / analytical
1	(0,0,0)	0.00	0	0	0
2	(0,0,1)	65.00	65.41	0.63	0.26
3	(0,0,2)	130.00	133.36	2.58	2.14
4	(0,0,3)	195.00	206.37	5.83	7.27
5	(0,0,4)	260.00	286.69	10.27	17.24
6	(0,0,5)	325.00	327.09	0.64	1.33
7	(0,1,0)	325.00	327.09	0.64	1.33
8	(1,0,0)	325.00	333.56	2.63	7.80
9	(0,1,1)	331.44	333.56	0.64	1.36
10	(1,0,1)	331.44	353.23	6.58	20.63
11	(0,1,2)	350.04	353.23	0.91	2.03
12	(1,0,2)	350.04	374.88	7.10	8.32
13	(0,1,3)	379.01	386.75	2.04	4.93
14	(1,0,3)	379.01	386.75	2.04	4.93
15	(0,0,6)	390.00	434.94	11.52	38.20
16	(0,1,4)	416.20	434.94	4.50	12.00
17	(1,0,4)	416.20	462.57	11.14	29.70
18	(0,0,7)	455.00	465.88	2.39	6.51
19	(0,1,5)	459.62	467.18	1.64	6.48
20	(1,0,5)	459.62	481.41	4.74	20.43

3.3. Hexahedrical acoustical cavity over a square plate

Ths system is modeled as a fluid-structure system. The plate is modeled through two-dimensional elements *CQUAD4*, with dimensions and material specified in section 3.1. The cavity is modeled with hexahedrical solid elements *CHEXA*, with dimensions and fluid properties specified in section 3.2.

The vertexes displacements of the plate are equal to zero. Then, the boundary conditions of the entire plate are u=v=r_z=0 and still in its vertexes z=0. The boundary conditions of the cavity are equivalent to rigid walls.

The adopted discretization results in a mesh of 64 two-dimensional elements of plate *CQUAD4* of four nodes each and 512 hexahedrical solid elements *CHEXA* of eight nodes each one, totaling 576 elements and 810 nodes.

The coupled frequencies obtained with the MSC.Nastran are shown in Tab. 3, where they are compared relative to the uncoupled ones. The average variation of the first thirty frequencies with predominance structural is -1.34Hz (-0.006%), for the frequencies with the fluid as the predominant medium is 0.92Hz (0.004%), and for all the frequencies is 0.091Hz (0.001%). The maximum value of the variation is -9.93 Hz (-0,03%).

Table 3. Predicted frequencies of the hexahedrical cavity over a square plate in Hz

Plate MSC.Nastran	Cavity MSC. Nastran	Decoupled mode	Coupled mode	Coupled MSC.Nastran	Coupled MEFLAB	Variation (%) coupled MEFLAB / MSC.Nastran	Variation Hz coupled MEFLAB - MSC.Nastran
	0	F1	1	0	0	0	0
34.41		S1	2	34.22	34.26	0.12	0.04
	65,41	F2	3	67.36	64.9	-3.65	-2.46
75,67		S2	4	75.22	75.66	0.58	0.44
75,67		S3	5	75.22	75.66	0.58	0.44
94,78		S4	6	94.55	93.79	-0.80	-0.76
	133,36	F3	7	134.17	133.16	-0.75	-1.01
191,56		S5	8	190.73	185.58	-2.70	-5.15
	206,37	F4	9	206.65	206.36	-0.14	-0.29
214,55		S6	10	214.4	210.63	-1.76	-3.77
252,84		S7	11	252.18	243.19	-3.56	-8.99
252,84		S8	12	252.18	243.19	-3.56	-8.99
	286,69	F5	13	287.23	286.56	-0.23	-0.67
	327,09	F6	14	327.24	327.05	-0.06	-0.19
	327,09	F7	15	327.24	327.05	-0.06	-0.19
343,86		S9	16	333.90	331.96	-0.58	-1.94
	333,56	F8	17	339.90	333.49	-0.12	-0.41
	333,56	F9	18	343.48	333.49	-2.91	-9.99
	353,23	F10	19	353.56	353.16	-0.11	-0.4
	353,23	F11	20	353.56	353.16	-0.11	-0.4
	374,88	F12	21	375.36	374.76	-0.16	-0.6
	386,75	F13	22	387.03	380.97	-1.57	-6.06
	386,75	F14	23	387.03	380.97	-1.57	-6.06
404,14		S10	24	403.54	386.61	-4.20	-16.93
404,14		S11	25	403.54	386.61	-4.20	-16.93
	434,94	F15	26	435.34	434.85	-0.11	-0.49
	434,94	F16	27	435.34	434.85	-0.11	-0.49
	462,57	F17	28	462.68	447.78	-3.22	-14.9
	465,88	F18	29	466.29	462.55	-0.80	-3.74
		F19	30	467.40	465.73	-0.36	-1.67

It is also verified in Table 3 the average variation of the first thirty coupled frequencies obtained by our finite element program MEFLAB relative to the decoupled ones obtained by the software MSC.Nastran; for frequencies with structural predominance it results -1,83%, for frequencies with predominance of the fluid medium it results -0,85% and for all of the frequencies it results-1,21%. The maximum absolute value of the variation is 16,93 Hz (4,20%) for the mode 24. This set of results displays the correspondence between MEFLAB and MSC.Nastran.

3.4. Structural mass minimization of the vibroacoustic system

Table 4 shows the natural frequencies before and after the mass optimization, where the thicknesses of the eight rows of the plate are the variables of the problem, as indicated in Tab. 5. The two constraints are relative to the minimum and maximum limits for the thickness, 0.01 in (0,0254 mm) and 1 in (25,4 mm) respectively, and the lower limit of 25 Hz for the second coupled natural frequency. As consequence, it is observed that the second coupled natural frequency decreases 9.21 Hz (26.9%).

Table 5 shows that thicknesses reduced on average 0.066 in (1.676 mm), equivalent to 33%. The maximum reduction is 0.091 in (2.314 mm) or 45.5%.

Table 4. Natural frequencies after mass optimization in Hz

Mode	Frequency before optimization	Frequency after optimization
1	0.00	0.00
2	34.22	25.01
3	67.36	52.67
4	75.22	55.63
5	75.22	60.75
6	94.56	67.91
7	134.18	134.22
8	190.73	134.43
9	206.65	145.76
10	214.41	150.27

Table 5. Variables for mass optimization

Variable	Original value	Optimized value
P1	0.2 pol (5.08 mm)	0.17718 pol (4.500mm)
P2	0.2 pol (5.08 mm)	0.10888 pol (2.765 mm)
P3	0.2 pol (5.08 mm)	0.12651 pol (3.213 mm)
P4	0.2 pol (5.08 mm)	0.12651 pol (3.213 mm)
P5	0.2 pol (5.08 mm)	0.12352 pol (3.137 mm)
P6	0.2 pol (5.08 mm)	0.10888 pol (2.765 mm)
P7	0.2 pol (5.08 mm)	0.17718 pol (4.500 mm)
P8	0.2 pol (5.08 mm)	0.12352 pol (3.137 mm)

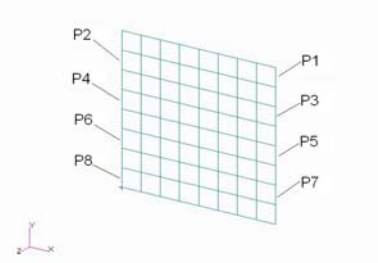

Fig. 4 shows the history of variables and objective function during the five iterations required for the optimization.

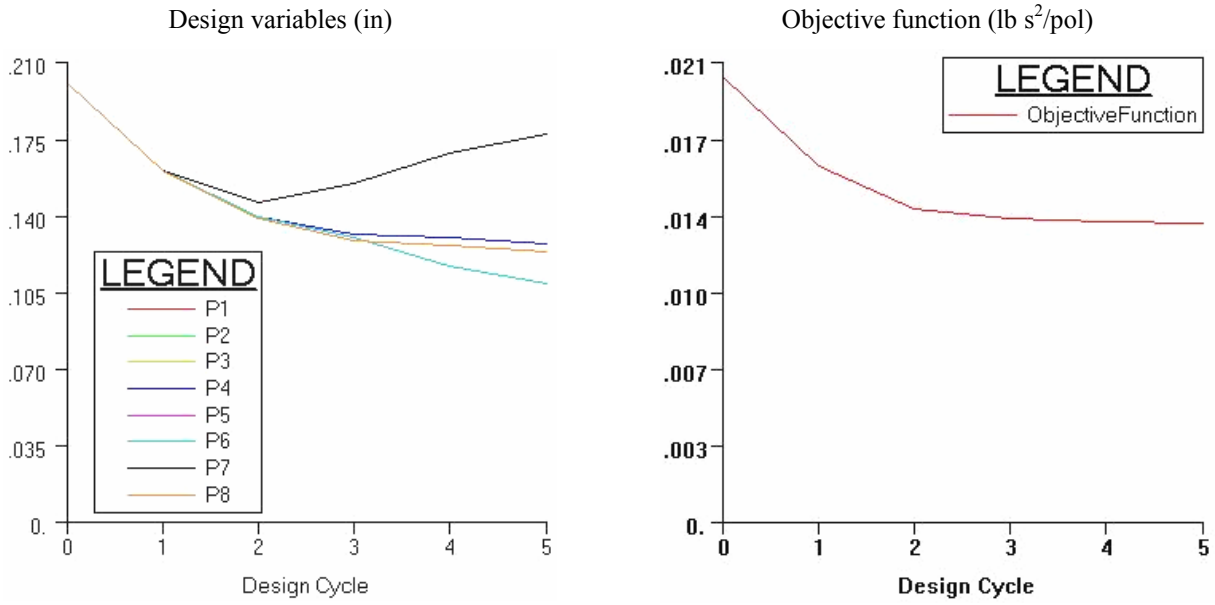

Figure 4. Iterations during the mass minimization

Table 6 shows the mass before and after the structural optimization. The structural mass reduces from 3.537 kg to 2.3706 kg, characterizing a reduction of 1.1664 kg (33%).

Figs. 5 and 6 show the modal shapes of modes 2, 3 and 4 of the coupled model as non-optimized and optimized respectively, being observed that the fringes of fluid pressure match the structural deformation in both cases. This serves to understand if the structure or the fluid predominates in the mode. From this consideration, it is observed that the third optimized coupled mode has the structure as predominant instead of the fluid, as can be seen in the non-optimized case. The third coupled frequency reduces from 67.36 to 52.67 Hz, meaning a variation of 14.69 Hz (21.81%).

Table 6 Mass of the system before and after the optimization.

Subsystem	Original volume in^3 (m^3)	Optimized volume in^3 (m^3)	Density $lb\ s^2/in^4$ (kg/m^3)	Original mass $lb\ s^2/in$ (kg)	Optimized mass $lb\ s^2/in$ (kg)
Fluid	40000 (0.655)	40000 (0.655)	1.27×10^{-7} (1.29)	0.057 (0.844)	0.057 (0.844)
Plate	80 (1.31×10^{-3})	53.609 (8.78×10^{-4})	2.65×10^{-4} (2700)	0.021 (3.537)	0.014 (2.370)
Total	40080 (0.657)	40053.609 (0.656)	---	0.078 (4.381)	0.071 (3.215)

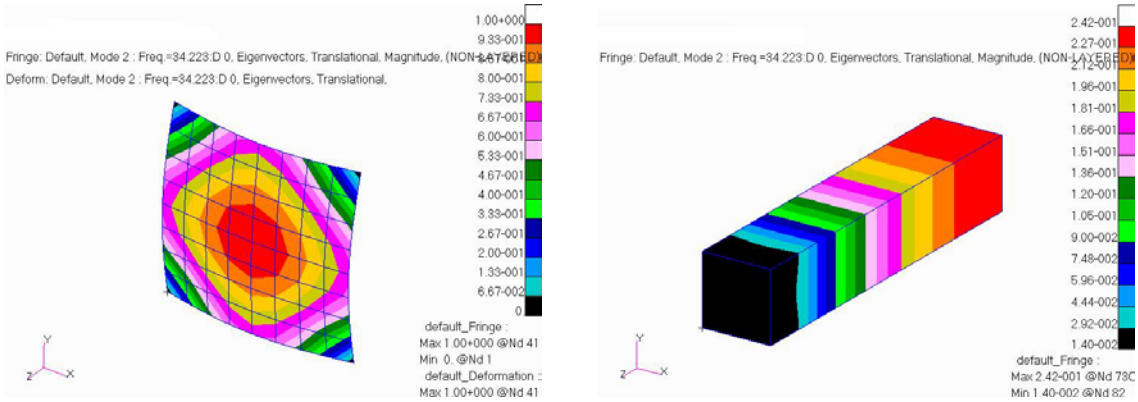

a) Structural deformation *b) Fringes of fluid pressure*

Mode 2: frequency 34.22 Hz, predominance of the structure.

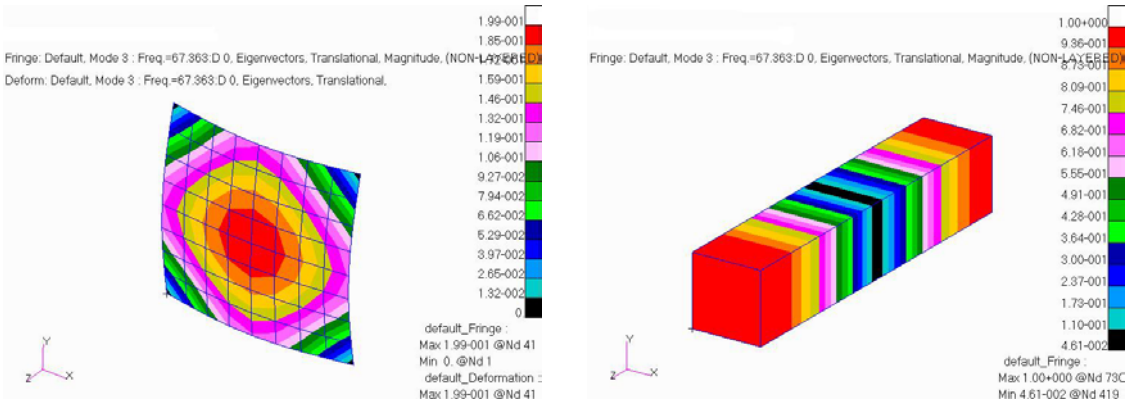

a) *Structural deformation* *b) Fringes of fluid pressure*

Mode 3: frequency 67.36 Hz, predominance of the fluid.

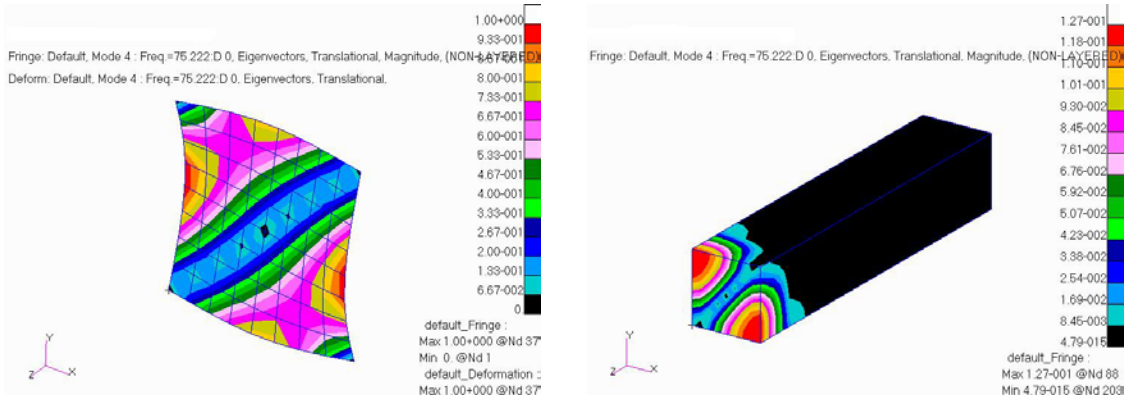

a) Structural deformation *b) Fringes of fluid pressure*

Mode 4: frequency 75.22 Hz, predominance of the structure.

Figure 5. Coupled modes before the optimization

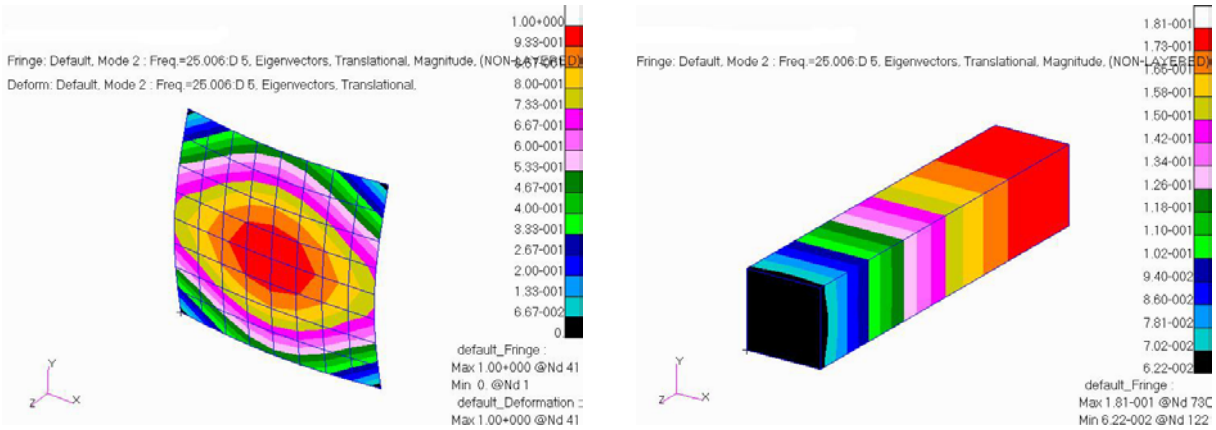

a) Structural deformation *b) Fringes of fluid pressure*

Mode 2: frequency 25.01 Hz, predominance of the structure.

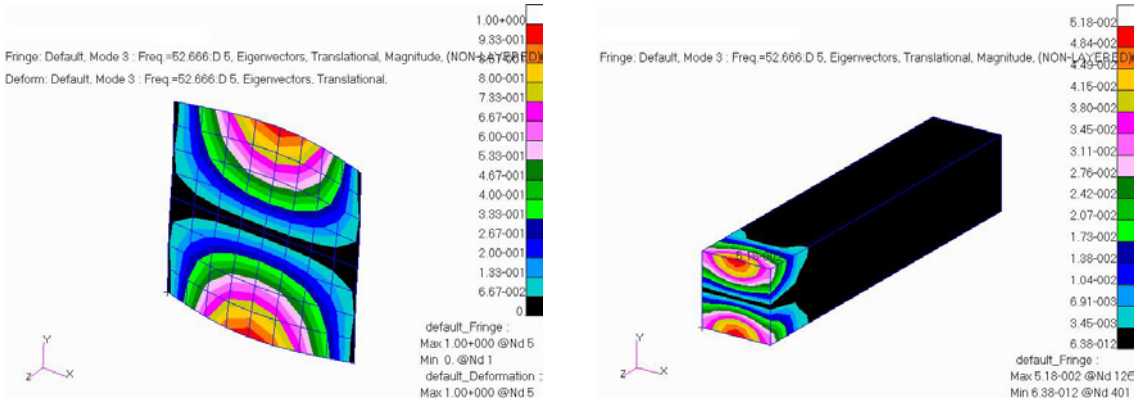

a) Structural deformation *b) Fringes of fluid pressure*

Mode 3: frequency 52.67 Hz, predominance of the structure.

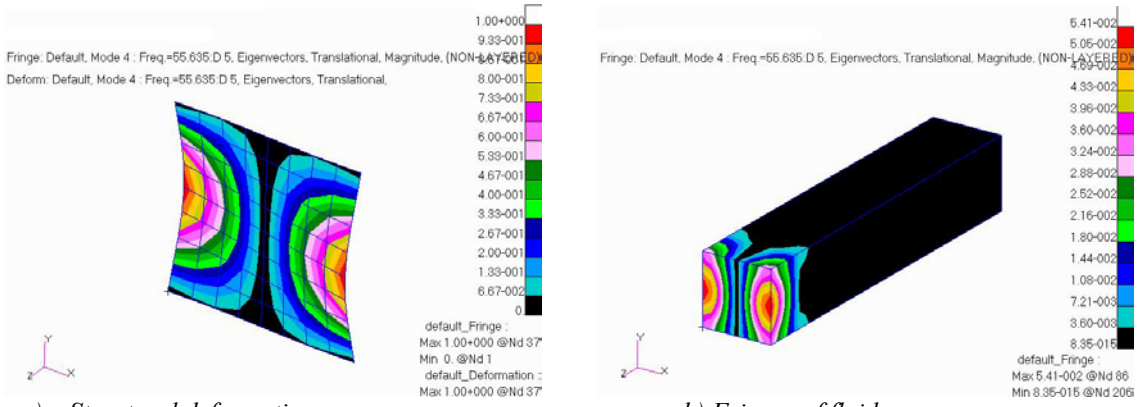

a) Structural deformation *b) Fringes of fluid pressure*

Mode 4: frequency 55.63 Hz, predominance of the structure.

Figure 6. Coupled modes after the optimization

4. CONCLUSIONS

The coupled natural frequencies of the system composed by a hexahedrical cavity on a square plate are compared with the decoupled frequencies, through the simulation in MSC.Nastran©. The average variation of the first thirty frequencies predominantly structural is -1.34%, for the frequencies predominantly fluid is 0.92%, and for all frequencies is 0.091%. The maximum variation value is -9.93 Hz.

During the mass minimization of the coupled system the structural mass decreases from 3.537 kg to 2.370 kg, characterizing a reduction of 1.166 kg (33%).

In a coupled system, the pressure fringes in the fluid match the structural shape deformation. This information and the decoupled frequencies values serve to infer if the structure or the fluid prevails in the coupled mode. If the fluid pressure fringes show a discontinuous behavior, probably the coupled mode is originated from the structural mode. If the structural deformation shows a discontinuous behavior, probably the coupled mode is originated from the fluid mode.

Once identified the original domain that drives the optimized coupled mode, it is possible to control better the coupled mode behavior due to some excitement.

5. ACKNOWLEDGEMENTS

The accomplishment of this work counted with some scientific research scholarship, BIC-FAPERGS (V.L.B.N.) and BIC-UFRGS (G.B.R.).

6. REFERENCES

Blevins, R. D., 1995, "Formulas for Natural Frequency and Mode Shape". Krieger Publishing Company.

De Mello, R., 2003, "Análise da Sensibilidade do Campo Acústico Veicular à Excitação do Sistema de Transmissão", Dissertação de Mestrado em Engenharia Mecânica, Universidade Federal de Santa Catarina, Florianópolis – SC, Brasil, 245 p.

Msc.Software, 1996. "NAS115 Fluid-Structure Analysis Using MSC.Nastran. Course Notes", The MacNeal-Schwendler Corporation.

Petyt, M. and Mirza, W. H., 1972, "Vibration of Column Supported Floor Slabs", Journal of Sound and Vibration, Vol. 21, pp. 355-364.

Reid, R. E., 1965, "Comparison of Methods in Calculating Frequencies of Corner Supported Rectangular Plates", NASA TN D-3030.

7. RESPONSIBILITY NOTICE

The authors are the only responsible for the printed material included in this paper.